

# LED Non-linear effects investigation in visible light communication via fuse transform approach with progressive learning algorithm based distortion

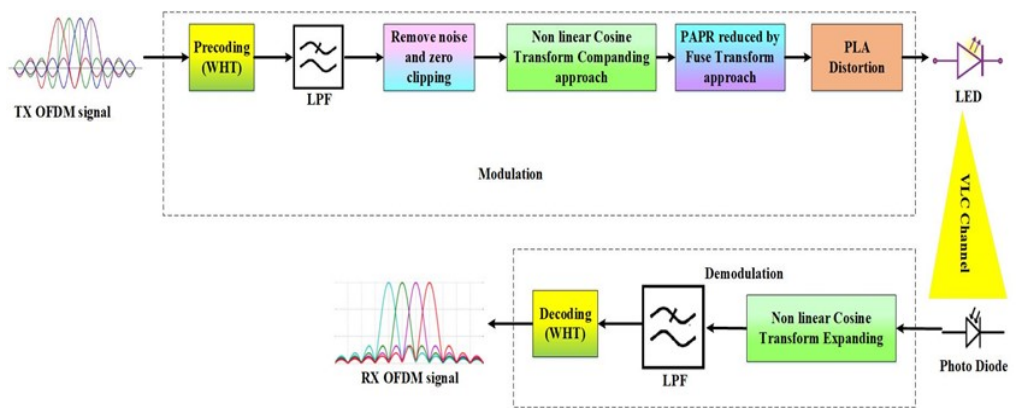
Sajitha Rani G.L.<sup>1\*</sup>, Vijayakumar N.<sup>2</sup>

<sup>1</sup>Department of Electronics and Communication Engineering, University College of Engineering, Kariavattom, Trivandrum, Kerala, India. <sup>2</sup>Department of Electronics and Communication Engineering, Government Engineering College Bartonhill, Trivandrum, India.

Received on: 22-Nov.-2022, Accepted and Published on: 14-Feb-2023

## ABSTRACT

Visible Light Communication (VLC) technology, which employs visible light modulation, broadly enables high-speed internet communication in the modern era. Due to its many advantages over conventional radio frequency, including a greater transmission rate, large bandwidth, low energy consumption, fewer health concerns, reduced interference, etc., VLC has recently grown in popularity. LEDs have drawn much attention for VLC implementation because of their exceptional qualities, including low cost and power consumption, but mainly because they can be utilized for lighting and communications. Moreover, LED modulation Scheme like OFDM leads to an excellent top-to-medium power ratio, including clipping with distortion. Here we report a novel Fuse Transform Approach with Progressive Learning Algorithm based Distortion in VLC to transmit the data, attenuate the excellent top-to-medium power ratio, including clipping and distortion, and investigate the LED non-linear effects of VLC.



**Keywords:** OFDM, LED, Visible light communication (VLC), PLA

## INTRODUCTION

Since then, several developments in telecommunication equipment have followed client requests for quicker and further responsible communication. There have been many paradigm shifts in wireless communication since the invention of the radio, and wireless telegraphy, including electromagnetic waves. Electromagnetic (EM) waves are used in a radio transmission to carry coded data.<sup>1</sup> Current society uses electromagnetic waves (EM

waves) for various purposes, such as radio broadcasting, Wi-Fi, mobile phone communication, health presentations, etc. EM waves could be divided into wireless, infrared, visible, ultraviolet, and other categories. Since radio frequency (RF) transmission happens at the rapidity of light, can't involve a medium of transmission, and cover great spaces, it is the most often used part of the electromagnetic spectrum (EM spectrum) for communication.

A line of sight between the sender and transceiver Bright light interference is also not a problem.<sup>2</sup> However, RF communication has some challenges, such as interference from cell phone use in aircraft. It affects navigation and messaging processes, causes limited bandwidth, safety concerns due to their ease of passing through walls, transmission power limitations due to potential threats to human survival, power inefficiency, etc.<sup>3</sup>

VLC (380 to 780 nm) was already created as an unusual solution to the abovementioned issue. The visible light spectrum band, also called VLC, and indoor infrared are addressed under the medium-range category (typically up to 10 km).<sup>4</sup> Wireless optical

\*Corresponding Author: Sajitha Rani G L, Kariavattom, Trivandrum, Kerala, India.  
Email: sajithaprem@gmail.com

Cite as: J. Integr. Sci. Technol., 2023, 11(3), 513.  
URN:NBN:sciencein.jist.2023.v11.513



©Authors CC4-NC-ND, ScienceIN ISSN: 2321-4635  
http://pubs.thesciencein.org/jist

communication equipment is focused on including a high-frequency bandwidth message range that is far wider than the current radio wireless networking frequencies. VLC is an OWC that provides localization, illumination, and communications using Light Emitting Diodes as light sources. VLC enables high data rates, low battery consumption, minimal latency, and sizeable unregulated bandwidth in wireless technologies.<sup>5,6</sup> An optical transmitter (Tx) and an optical receiver (Rx) make up the two components of VLC. Following pre-processing and encrypting, a binary bit stream powers the light source (LED/LD), and modulation transforms electrical impulses into optical communication systems. Pre-processing makes up for the signal distortion that other channels have generated. The equalization technique could enhance the LED's response frequency and transfer data rate. The transmitter's post-equalization can compensate for channel risks, like phase noise. Unfortunately, there are two significant problems with the LEDs utilized in VLC. First, bandwidth is constrained by the low-pass quality of LEDs. It has historically become the main challenge connected to VLC.<sup>7</sup> High-order coding modulation schemes were used to increase transmission rate with spectrum efficiency. A popular, promising technology for VLC networks is orthogonal frequency division multiplexing (OFDM) that have excellent spectral efficiency and is resistant to multipath propagation.

Asymmetrically clipped optical OFDM (ACO-OFDM) with DC-biased optical OFDM (DCO-OFDM) are the two variants of OFDM for VLC systems.<sup>8,9</sup> By zero-clipping the new bipolar OFDM signal while broadcasting just the optimistic works, ACO-OFDM transforms the transmitted data into a positive signal. In DCO-OFDM, the signal is transformed optimally using a DC bias. Only the odd subcarriers transmit information bits in ACO-OFDM, while all subcarriers do so in DCO-OFDM. DCO-OFDM may be less efficient than ACO-OFDM in terms of median optical power. DCO-OFDM is less effective in order of bandwidth than ACO-OFDM since it utilizes just half of the sub-carriers for file transfer.<sup>10</sup> Higher-order modulation schemes like OFDM have effectively solved this problem, which offers increased spectrum efficiency.<sup>11,12</sup> Digital signal processing methods, such as equalizers and classifiers using ANN, have also achieved data speeds in the Gb/s range.<sup>13,14</sup> The non-linearity in the electro-optic frequency response is a difficulty with LED-based technology, which is a complication since the waves are intensity-modulated onto the optical signal.<sup>15</sup> Because OFDM networks have many independent random sinusoids, they get a large peak-to-average power ratio (PAPR). It is problematic when working with non-linear transfer functions with digital-to-analogue converters. As a result, in incorrectly designed OFDM-based VLC systems, the received signal suffers from significant distortions.<sup>16</sup>

LED-based locating systems have gained popularity recently. Instead of RF, these technologies use visible light signals. Before that, VLC<sup>17</sup> was a particularly intriguing application of LED that was well-known in the communication sector. LED tilting is demonstrated for the first time, demonstrating its potential to increase positioning precision in VLCs (PA). The positioning technique used, the precision of the VLP structure for a single PD-based static Rx, and how reflections affect accuracy using the

received signal from mutual LoS and NLoS transmission pathways are all demonstrated.<sup>18</sup>

Furthermore, modulation techniques like orthogonal frequency-division multiplexing (OFDM) take a tremendous peak-to-average power ratio because of clipping and distortion. To examine the impacts of LED non-linearity on VLC, lower the peak-to-average power ratio, and deterministically disseminate the information. Hence, the Fuse-transform Approach with Progressive Learning Algorithm proposed is based on system architecture distortion to mitigate the issues in VLC.

The article follows: Section I depicts the Introduction, Section II represents the related works in previous methods, Section III depicts the Fuse Transform Approach with Progressive Learning Algorithm in VLC, Section IV gives the output of the Simulation Process, and Section V concludes this paper.

## RELATED WORKS

A novel channel access model for VLC, the CSK hopping pattern concept, was presented by W.X. Hong et al.<sup>19</sup> In this study, the transmitter loads data using the CSK hopping pattern model into LEDs. The network access point with LEDs for illumination was then built, and VLC systems may be identified by their distinctive colour patterns. When a transceiver spots a specific colour scheme in the illuminated coverage region, the created model connects to the access point through an interaction access network process. The developed CSK hopping pattern model significantly reduces the terminal access network delay and interruption among nearby access points. However, with the created CSK hopping pattern model, it was challenging to reconcile communication and lighting.

High-Brightness LEDs (HB-LEDs) were used in these systems by Sebastián et al.<sup>20</sup> used High-Brightness LEDs (HB-LEDs) to transmit data by quickly altering the intensity of the produced light and employing them as lighting sources. The significant problem is that VLC provides a rapid HB-LED driver to reproduce the target light-intensity waveforms containing elements as high as a few MHz. The HB-LED drivers, however, that have been presented thus far rely on utilizing an RF Power Amplifier (RFPA). These technologies have high power losses even when they provide the required speed. This work proposes several approaches based on rapid-reaction DC/DC converters to overcome this limitation. As a result, many DC/DC conversions are being investigated to either be used in place of or help an RFPA reach maximum performance.

The underwater VLC system Wang et al.<sup>21</sup> proposed uses QAM-DMT and Multi-PIN reception to accept MRC. The transmitter was a silicon substrate LED with a green emission peaking at  $\mu\text{m} \times 600 \mu\text{m}$  with a peak emission wavelength of 521 nm. The VLC structure's BER performance was investigated of the LED's quiescent working point, zero-padding number, and ISFA tap number, with the proportion of two receivers. It is noted that the proportion of two receivers might significantly impact the method's effectiveness. The most effective data rate of the method can reach 2.175 Gb/s, according to a study that also examined the BER performance vs the bandwidth of the signal in 32QAM, 64QAM, and 128QAM modulation formats. According to research knowledge, this VLC system uses a PIN receiver, and commercial LEDs achieved the highest data throughput in pure water.

Wu et al.<sup>22</sup> looked at the effectiveness of the Gaussian mixture model (GMM) and K-means classification procedures under highly non-linear circumstances. The findings demonstrate that the signal peak-to-peak voltage range when using GMM is roughly 0.25 V, which exceeds the area when using K-means at a data rate of 1.5 Gbps while meeting the BER criterion of forward error correction.

A hybrid PAPR decrease method depends on clipping and signal transformation was presented by Freag et al.<sup>23</sup> Utilizing the Hadamard transform, the suggested solution lowers the PAPR without impacting the bit error rate (BER) of the VLC methods. Additionally, it establishes the optimal clipping threshold, below which the PAPR is decreased, and the BER of the VLC organisms is increased. Utilizing BER and an additional cumulative distribution function, the effectiveness of the suggested system is evaluated.

To reduce the peak-to-average power ratio (PAPR) for direct current-biased optical orthogonal frequency division multiplexing (DCO-OFDM) VLC systems, Hu et al.<sup>24</sup> introduced a unique PAPR reduction approach. Low complexity applicant building and the absence of side information (SI) transfer are two advantages of this system. The suggested method comprises linearly merging time domain even or odd patterns with cyclic shift and phase rotation to get the candidates. Even or odd series is created by performing an inverse fast Fourier transform on the signal's even then odd elements, respectively. Additionally, a deterministic but efficient choice mechanism of cyclic shift with phase rotation is devised, enabling the receiver to retrieve the transmitted candidate signal without SI. It makes every candidate distinct and thus enhances PAPR reduction efficacy.

To reduce the PAPR of an OFDM-based VLC system, Ahmad et al.<sup>25</sup> proposed a novel modulation method that combines discrete Fourier transform (DFT) precoding with Gaussian minimum shift keying (GMSK) pulse shaping. The notion of group precoding is also introduced to handle the rising complexity of the DFT precoding system.

Ma et al.<sup>26</sup> have analyzed that the appearance of a VLC organization can be considerably hampered by the non-linear effects caused by various components, including electrical amplifiers and optoelectronic devices. This research proposed a clustering procedure established on k-means in VLC methods to reduce the effects of non-linear distortion with the bit error rate (BER) can be diminished from  $2.4 \times 10^{-1}$  to  $3.6 \times 10^{-3}$ .

Lain et al.<sup>27</sup> discussed the signal distortion owing to LED non-linearity that happens during the electrical-to-optical conversion process in VLC, causing a reduction in the performance of the VLC system. It was suggested to use ANN pre-distortion to account for LED non-linearity because ANNs are regarded to be able to approximate any function. The corresponding restrictions in the intended ANN pre-distorter might be dynamically adjusted to monitor the LED time-variant characteristics caused by temperature difference with ageing without requiring further training sequences using a backup copy of the original electrical source.

Abd Elkarim et al.<sup>28</sup> examined LEDs; however, authors have non-linear impacts on the transferred signal and harm system performance, particularly in multicarrier modulation systems. This

study examined the layered asymmetrically clipped optical, orthogonal frequency division multiplexing (LACO-OFDM) and the effects of LED non-linearity on application performance. The impact of the second-order non-linear distortion in contrast to the clipping noise is supplied and then studied over a range of power levels and non-linearity intensities. The system performance is investigated with various layers and a non-linear LED model.

## FUSE TRANSFORM APPROACH WITH PROGRESSIVE LEARNING ALGORITHM IN VISIBLE LIGHT COMMUNICATION

VLC is generally used for many things, such as internal communications infrastructure, localization connections, automotive, and underwater communications systems. A sender and a transmitter are the two main parts of the VLC network. To transmit information, a transmitter made of an LED modulates the light's intensity. In contrast, photo sensors at the recipient portion capture light and convert it into data streams. In the VLC system, LEDs emit light while reducing the emission angle employing their field of view. This technique relies on the sightline between the sender and receiver to function. Light-emitting diodes, widely used in VLC networks, generally have a non-linear electro-optic output. It is particularly problematic when using cutting-edge modulation schemes like orthogonal frequency-division multiplexing (OFDM), which has a large peak-to-average power ratio because of clipping and distortion. Hence, a novel Fuse-Transform Technique was proposed that utilizes a unitary matrix which amalgamates the Non-Linear Cosine Transform Companding Approach. And also, the Walsh-Hadamard transform to the System integration to computationally disperse the information and minimize the peak-to-average power ratio—consequently, Progressive Learning Algorithm-based distortion to examine the LED Non-linearity effect on VLC.

### WALSH-HADAMARD TRANSFORM(WHT)

The WHT transforms a signal into a set of orthogonal, rectangular waveforms identified as Walsh functions using a genuine, non-sinusoidal conversion. The Walsh-Hadamard matrix is produced by arranging the rows of Hadamard matrices in a specific manner.  $W_M$  is the Hadamard matrix with elements 1 or -1. The Hadamard matrix of orders 1, 2, and  $2M$  is computed as

$$W_1 = [1]; W_2 = \frac{1}{\sqrt{2}} \begin{bmatrix} 1 & 1 \\ 1 & -1 \end{bmatrix}; W_{2M} = \frac{1}{\sqrt{2M}} \begin{bmatrix} W_M & W_M \\ W_M & W_{-M} \end{bmatrix}$$

Where  $W_M$  is the Complementary of  $W_{-M}$ .

The element of the WHT matrix could generally be expressed as

$$W_{y,v} = (-1)^{\sum_j^{m-1} y_j v_j} \quad (1)$$

Where  $m = \log_2 M$ ,  $y$  and  $v$  are the rows with columns position in the WHT matrix and  $y_i * v_i$  is the  $i$ th product operation of bit-by-bit for the binary number, which characterizes the integer amounts  $y$ ,  $v$  and  $m$ ; -1 is the sum of binary digits in every index.

## NON-LINEAR COSINE TRANSFORM COMPANDING APPROACH(NCT)

The cosine transform function can describe a finite stream of document sets as the summation of cosine functions vibrating at variable frequencies. A specific type of Fourier-related Transform called a CT only uses a substantial portion. Additionally, as CT is a true transformation and data mapping is a fact, the in-phase/quadrature-phase (IQ) imbalance would be reduced by combining CT with the OFDM technique. The carrier frequency offset also has a negligible effect on the CT than the FFT. The CT matrix could be shown as follows:

$$CT_{a,n} = \sqrt{\frac{2}{N}} \sum_{n=0}^{M-1} \varphi_n \cos \left[ \frac{\pi(2a+1)n}{2M} \right] \quad (2)$$

where  $\varphi_n$  is the normalization factor, and k & n are the positions of the rows and columns in the DCT matrix.

$$\varphi_n = \left\{ \begin{array}{ll} \frac{1}{\sqrt{2}}, & n = 0 \\ 1, & 0 < n < M - 1 \end{array} \right\} \quad (3)$$

## $\pi$ -LAW COMPANDING APPROACH

It is possible to acquire the compressor feature in the  $\pi$ -law companding information, which consists of a linear segment for low-level inputs and a logarithmic segment for advanced inputs. It is suppressed at the transmitter to reconstruct the signals and then prolonged at the receiver.

$$X_c(n) = K_{max} \frac{\log(1 + \pi |\bar{X}(n)| / K_{max})}{\log(1 + \pi)} \text{sgn}[\bar{X}(n)] \quad (4)$$

Where  $K_{max} = \max(\bar{X}(n))$ ,  $n = 0, 1, \dots, M - 1$ .  $\pi$  is a companding factor which could be used to regulate the PAPR reduction's intensity.  $X_c(n)$  is the combined sample.  $\bar{X}(n)$  is the original sample. The expansion is the reverse of equation (4), as given below

$$\hat{X}(n) = \frac{K_{max}}{\pi} \left[ \exp \left[ \frac{|X_c(n)| \ln(1 + \pi)}{K_{max}} \right] \right] \text{sgn}[A_c(n)] \quad (5)$$

Where  $\hat{X}(n)$  is the test that was expanded and calculated.

## $\beta$ -LAW COMPANDING APPROACH

This approach might lessen the PAPR, which is the main flaw with OFDM.

$$b(a) = \left\{ \begin{array}{ll} b_{max} \frac{\beta^{-|a|}}{(1+\beta)} \text{sgn}(a), & 0 < \frac{|a|}{a_{max}} \leq \frac{1}{\beta} \\ b_{max} \frac{[1 + \log_e \beta^{-|a|}]}{(1 + \log_e \beta)} \text{sgn}(a), & \frac{1}{\beta} < \frac{|a|}{a_{max}} \leq 1 \end{array} \right. \quad (6)$$

Where a is the input signal, b is the output signal, and  $\beta$  is the Companding factor.

## COS COMPANDING APPROACH

At the transmitter, the signal is compacted, and the subsequent expanding processing is employed to rebuild it at the receiver. The compression function is given as follows

$$g(y) = \text{sgn}(y) \sqrt[2]{\gamma \left[ 1 - \cos \left( -\frac{|y|}{\sigma} \right) \right]} \quad (7)$$

Where  $g(y)$  is the compressed signal;  $z$  is the compression parameter;  $\text{sgn}(y)$  is the sign function, and  $\sigma$  is the standard deviation of the input signal  $|y|$ .

The decomposition process on the recipient side uses the inverse function  $g(y)$ .

$$g^{-1}(y) = \text{sgn}(y) \left| -\sigma \gamma \cos \left( 1 - \frac{|y|^{2z}}{\gamma} \right) \right| \quad (8)$$

The mean power of output values is controlled by the positive constant to conserve having a similar mean power ratio among the input with output signals  $\gamma$ .

$$\gamma = \left( \frac{E[|y|^2]}{E^d \sqrt{\left[ 1 - \exp \left( -\frac{|y|}{\sigma} \right) \right]^2}} \right)^{\frac{z}{2}} \quad (9)$$

Where d is the companding degree.

## FUSE-TRANSFORM APPROACH

Additionally, both transforms, such as Walsh Hadamard and Non-linear Cosine transform, were combined into a single transform to diminish complexity and peak-to-mean power ratio.

$$F_{m \times n} = [(NCT_{m \times n})^{\wedge}] \{[(WHT_{m \times n})^{\wedge}]^T\} \quad (10)$$

Where  $(.)^{\wedge}$  depicts the bit-reversed order and  $(.)^T$  depicts the transposition. The actual orthonormal matrix CT's inverse and transpose were identical.

$$ICT = CT^{\wedge} \quad (11)$$

CT probably had a diagonal block arrangement (DBS). Therefore, fewer additions and multiplications were possible since more than 65% of its parts were zero. It was, therefore, helpful in lowering the PAPR and the M-class matrix.

AWGN was additional to the accepted information before serial-to-parallel conversion with zero padding elimination on the receiver side  $y(t)$ . This information was then added to the Fuse Transform accordingly. The modulation alphabet was then removed from the output. The LED electro-optic transfer function, several bias points, as well as the ascertained AC value were all used in this investigation. The LED was operated in a quasi-linear section for its feature around the selected bias point with AC level, and the BERs of the output signal were checked to determine the distortion levels. Therefore, this led to a greater comprehension of the ideal bias circumstances.

## PROGRESSIVE LEARNING ALGORITHM(PLA) BASED DISTORTION FOR NON-LINEAR EFFECT IN VLC

This approach uses the non-linear properties of the LED and designs the distorter for a VLC system based on those non-linear properties. The distorter's non-linear properties are inverse to those of an LED. The output signal should ideally be linear when this distorter is cascaded with a non-linear LED.

A non-linear polynomial description of the distortion, which is theoretically described as



$$\hat{u}(k) = \sum_{m=0}^{M-1} \hat{g}_m a^{m+1}(k) \quad (12)$$

Where  $\hat{u}(k)$  is the distorted output of the input signal  $a(k)$ ,  $\hat{g}_m$  are the coefficient, and M is the non-linearity order. At first, the coefficient  $\hat{g}_0$  is set to unity as well as the residual coefficients ( $\hat{g}_1, \hat{g}_2 \dots \dots, \hat{g}_m$ ) are set to zero. Subsequently, based on the non-linear features of LED, the values of these coefficients would be amended. The PLA-based distortion is used to evaluate their values. This process is a two-step procedure. Coefficient evaluation, which depends on the initial selection but is discussed in the following subsets, comes after fault detection and decision-making. Figure 1 explains the flow chart for PLA-based distorter.

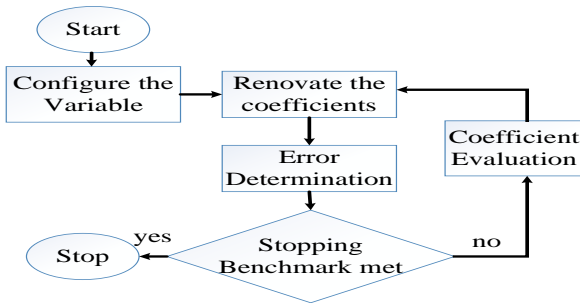


Figure 1: Flow chart for PLA-based distorter

**ERROR DETERMINATION AND DECISION MAKING**

A  $k$  is primarily generated and passed through a PLA-based distorter. The distorted signal  $\hat{u}(k)$  is then transmitted over the LED after the distorter, where it radiates a non-linear optical power signal  $P_{out}$ .

$$P_{out} = \sum_{n=0}^{\infty} h_n (I_{in}(t) - I_{DC})^n \quad (13)$$

Where  $P_{out}$  is the LED's optical power emission,  $I_{in}(t)$  is the input current signal and  $I_{DC}$  is the LED's normalized bias voltage, while  $h_n$  is the nth-order non-linearity coefficient. Since the second-order term encompasses the majority of the non-linearity in LEDs, Eq (13) is limited to the second-order term given as

$$P_{out} = h_0 + h_1(I_{in}(t) - I_{DC}) + h_2(I_{in}(t) - I_{DC})^2 \quad (14)$$

and the coefficients  $h_0, h_1$  and  $h_2$  can be defined as  $h_0 = \tau, h_1 = 1, h_2 = -4\tau + 2$

where  $\tau$  handles the cruelty of the non-linearity. To measure error, this optical power signal  $P_{out}$  is transformed into an electrical signal  $b(k)$  using an optical-to-electrical converter (OEC). To calculate the error expressed in EVM, the electrical equivalents of the input signal,  $a(k)$ , and the LED output signal,  $b(k)$ , are compared. This comparison is made to determine the error.

$$EVM = \frac{\sqrt{\frac{1}{P} \sum_{n=0}^{P-1} ((I(b_n) - I(a_n))^2 + (Q(b_n) - Q(a_n))^2)}}{\sqrt{\frac{1}{P} \sum_{n=0}^{P-1} ((I(a_n))^2 + (Q(a_n))^2)}} \quad (15)$$

where  $I(b_n)$  and  $Q(b_n)$  are the recorded signal's in-phase and quadrature-phase components at the nth subcarrier  $b(k)$  and  $I(a_n)$  and  $Q(a_n)$  are the in-phase and quadrature-phase components at the nth subcarrier of the input signal  $a(k)$ .

The first stage of the method is completed by comparing the measured EVM to the threshold EVM (EVMT) for decision-making. The QoS requirements of an OFDM-based VLC organism often determine the value of EVMT. The intended bit error rate (BER) or signal-to-noise ratio (SNR) can be used to compute it. No additional coefficient evaluation is needed if the observed EVM is less than the EVMT and the output signal is linear. The coefficients of the distorter are re-estimated if the EVM is higher than the EVMT (indicating that the LED output signal is non-linear). Recalculating the distorter coefficients may be necessary if the EVM changes due to an alteration in the input signal, a variation in the physical characteristics of the LED, or both.

**COEFFICIENT EVALUATION**

The outcome of the initial phase's decision influences the algorithm's second step. The fault among the input power  $b(k)$  and the output signal  $u(k)$  is decreased. Similar to the polynomial model used to evaluate the distorter, that can be described as

$$u(k) = \sum_{m=0}^{M-1} g_m b^{m+1}(k) \quad (16)$$

$$= \begin{bmatrix} b(0) & b^2(0) & \dots & b^m(0) \\ b(1) & b^2(1) & \dots & b^m(1) \\ \vdots & \vdots & \ddots & \vdots \\ b(P-1) & b^2(P-1) & \dots & b^m(P-1) \end{bmatrix} \begin{bmatrix} g_0 \\ g_1 \\ \vdots \\ g_{M-1} \end{bmatrix}$$

$$u = Bg \quad (17)$$

where gm stands for the coefficients evaluated here, the coefficient evaluation block's incoming and outgoing signals are represented by  $b(k)$  and  $u(k)$ , respectively, and M is the non-linearity order, the same as the PLA-based distorter.

For an overall sample count of P, 'u' is an output vector of length  $P \times 1$ , B is an input matrix of length  $P \times M$ , and g is an output vector of length  $M \times 1$ . Since it is an overdetermined system, there is no solution. On the other hand, the coefficient vector g can be evaluated using the least square (LS) approach, which is shown as follows:

$$\hat{g} = \arg \min \|u - Bg\|^2 \quad (18)$$

The solution of the above equation is given as

$$\hat{g} = (B^H B)^{-1} B^H u \quad (19)$$

These parameter estimates are used as the distorter parameters to saturate the incoming signal with distortion before receiving the linearized output signal from the LED. The proposed PLA-based system's algorithm gives a summary of the actions above.

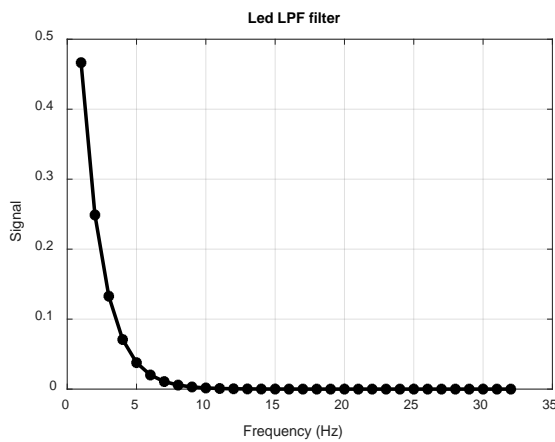
**PLA Based Algorithm**

1. Input: OFDM signal  $a(k)$
2. Initialization:  $\hat{g}_0 \leftarrow 1; \hat{g}_1, \hat{g}_2, \dots \dots \hat{g}_m \leftarrow 0$
3. Evaluate PLA-based distorter output  $\hat{u}(k)$  using Equation(12)
4. Evaluate LED output  $b(k)$  and OEC
5. Evaluate EVM using equation (15)
6. while  $EVM > EVMT$  do
7. Calculate the coefficient values  $g_m$  using equation (19)
8. end
9. System is Linearized

**SIMULATION RESULTS AND DISCUSSION**

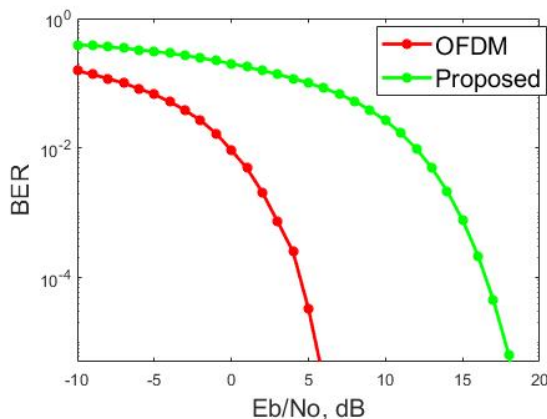
**SIMULATION RESULTS**

This unit illustrates the implementation results and compares the outcomes of the proposed method. The Proposed method is simulated via MATLAB R2021a on Intel(R)core(TM)i5 10400 CPU@2.66 GHz, 4 GB RAM.



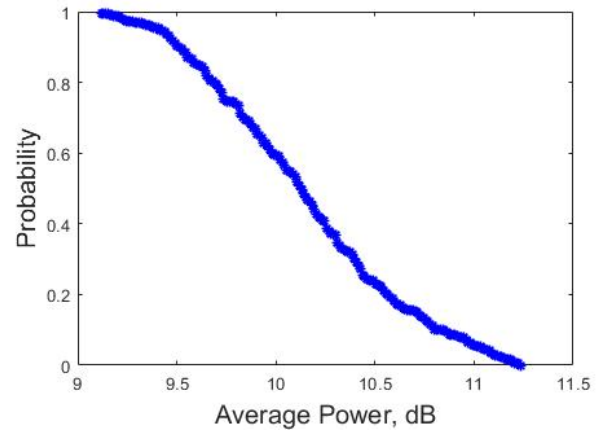
**Figure 2:** LED output for signal vs frequency

Figure 2 represents the linearity graph for the proposed method. This graph reveals that a low pass filter will pre-process the signal for noise removal based on the proposed fuse transform with the PLA method, which achieves high for low frequency; if the frequency increases, the signal will attain low. Finally, the proposed method removed the noise and unwanted frequency in the VLC.



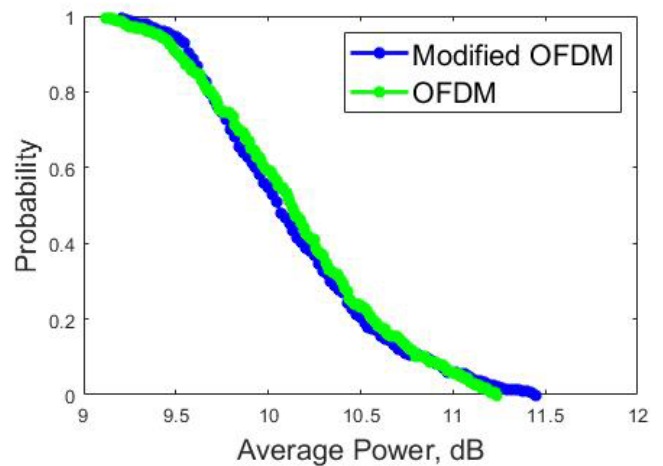
**Figure 3:** BER performance as a function of Eb/No

Figure 3 emphasizes that the BER should be noted that the BER objective was not met for most of the various bias point values in the conventional OFDM method. But the proposed approach BER performance was significantly improved, with all BER curves meeting the BER objective at the high Eb/No. The near coherence between the BER curves for Eb/No ratios greater than 10 dB, the resultant BER curves increasingly diverge with increasing Eb/No, indicating that an improvement in the frequency offset raises the BER value at a fixed Eb/No ratio. Compared to the conventional method, the BER performance of the Proposed fuse transform with the PLA approach achieves high performance.



**Figure 4:** Probability vs Average power

Figure 4 represents the Proposed fuse transform with PLA probability vs average power. This graph reveals that the probability will attain a high value when the average power is low. If further increasing the power value, the probability deteriorates the performance.



**Figure 5:** Probability vs Average power for Modified OFDM

Figure 5 shows that the average power performance, when applied to the proposed fuse transform with the PLA approach, will be truncated if a high probability is reached. Compared with conventional OFDM, the probability degrades the performances with power value, but the Modified OFDM achieves a high average power with less probability.

## COMPARISON RESULTS

The performance of the Fuse-transform Approach with PLA-based distortion is discussed with a previous method, such as C-OFDM, F-OFDM and ACO-OFDM, DCO-OFDM and OFDM, respectively.

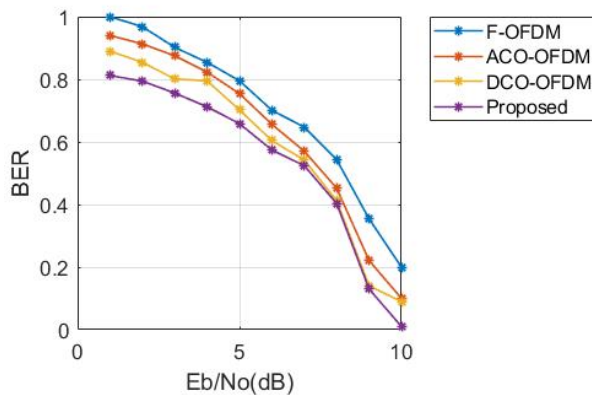


Figure 6: Plot between BER and  $E_b/N_0$

Figure 6 represents the  $E_b/N_0$  increases the proposed method achieves the BER with secure data transmission. The probability of BER performance is compared when the proposed approach is put up against earlier methods like F-OFDM, ACO-OFDM, and DCO-OFDM, respectively. The proposed approach attained low when compared to a prior method, such as F-OFDM has 0.2, ACO-OFDM has 0.18, and DCO-OFDM has 0.1. The BER of the proposed method achieves minimum error compared to another prior method.

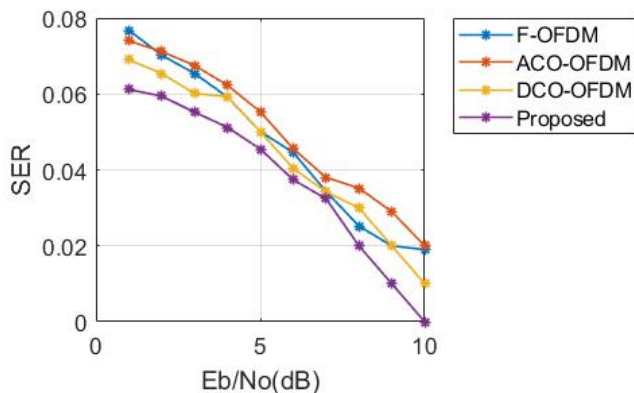


Figure 7: Plot between SER and  $E_b/N_0$

A VLC network with different non-linear LEDs behaves drastically different in terms of SER. However, as shown in Figure 7, the SER performance of the OFDM VLC structure employing different non-linear LEDs in the incidence of the PLA-based distorter approaches that of the linear VLC system. And comparing the benchmark efficiency to the performance of the VLC structure with distorter-LED shows that the PLA-based distortion method adjusts to some modification in the non-linearities of LED. Additionally, the performance of the linear VLC structure and the non-linear VLC structure with a PLA-based distorter is nearly equivalent. The proposed method is compared to the prior method and attained less SER when compared to a prior method, such as F-

OFDM has 0.02, ACO-OFDM has 0.02, and DCO-OFDM attained 0.01 with 10db of  $E_b/N_0$ .

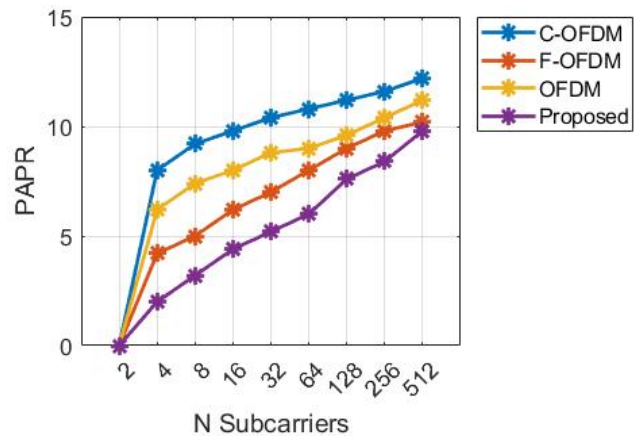


Figure 8: Plot between PAPR and N subcarriers

Figure 8 depicts that Subcarriers increase in the proposed method decreases with peak to average power ratio compared to a conventional method such as F-OFDM, C-OFDM and OFDM, respectively. When the subcarriers increase from fair values such as 2, 4, 8,....., N carriers, the PAPR achieves the minimum reduction when compared with the prior method attained C-OFDM as 9, F-OFDM as six and OFDM as 4.

The proposed method was compared with C-OFDM, F-OFDM and OFDM. The peak-to-average power ratio reduced from approximately 12 to 3, the BER attained less value with secure information, and the LED's non-linearity effect achieved linear visible light communication.

## CONCLUSION

In our study, orthogonal frequency division multiplexing raises the electro-optic output of the light-emitting diode, increasing the quick peak-to-mean power ratio, which reasons clipping and distortion in VLC. Finally, a novel Fuse Transform Approach was proposed, incorporating the Non-Linear Cosine Transform Companding Approach. And also, the Walsh-Hadamard transform deterministically distributed the information, mitigated the peak to average power ratio, and Progressive Learning Algorithm based distortion examined the LED Non-linearity effects on VLC attained the linearity with 96%.

## REFERENCES

1. S.U. Rehman, S. Ullah, P.H.J. Chong, S. Yongchareon, D. Komosny. Visible light communication: a system perspective - overview and challenges. *Sensors* **2019**, 19(5), 1153.
2. K. James Singh, Y.M. Huang, T. Ahmed, A.C. Liu, S.W. Huang Chen, F.J. Liou, H.C. Kuo. Micro-LED as a promising candidate for high-speed visible light communication. *Applied Sciences* **2020**, 10(20), 7384.
3. S.N. Ismail, M.H. Salih. A review of visible light communication (VLC) technology. In *AIP Conference Proceedings* **2020**, 2213(1), 020289, AIP Publishing LLC.
4. L.E.M. Matheus, A.B. Vieira, L.F. Vieira, M.A. Vieira & O. Gnawali. Visible light communication: concepts, applications and challenges. *IEEE Communications Surveys & Tutorials* **2019**, 21(4), 3204-3237.

5. Z. Geng, F.N. Khan, X. Guan, Y. Dong. Advances in Visible Light Communication Technologies and Applications. *Photonics*, **2022**, 9(12), 893.
6. S. Sun, F. Yang, J. Song, Z. Han.. Joint resource management for intelligent reflecting surface-aided visible light communications. *IEEE Transactions on Wireless Communications*, **2022**, 21(8), 6508-6522.
7. P.A. Haigh, Visible Light: Data Communications and Applications; IOP: London, UK, 2020. <https://iopscience.iop.org/book/mono/978-0-7503-1680-4>
8. J. Pradhan, P. Holey, V.K. Kappala, S.K. Das. Performance analysis of ACO-OFDM NOMA for VLC communication. *Optical and Quantum Electronics* **2022**, 54(8), 1-16.
9. S. Vappangi, V.V. Mani. Impact of STO and STO-estimation in DST-DCO-OFDM-based visible light communication systems. *ICT Express*, **2022**, 8(3), 414-418.
10. S.M. Hameed, S.M. Abdulsatar & AA Sabri, BER comparison and enhancement of different optical OFDM for VLC. *Int. J. Intelligent Engineering and Systems* **2021**, 14(4), 326-336.
11. J. Abdulwali, S. Boussakta. Visible Light Communication: An Investigation of LED Non-Linearity Effects on VLC Utilising C-OFDM. *Photonics*, **2022**, 9(3), 92.
12. R. Bian, I. Tavakkolnia & H. Haas. 15.73 Gb/s visible light communication with off-the-shelf LEDs. *J. Lightwave Technol.*, **2019**, 37(10), 2418-2424.
13. F. Hu, S. Chen, Y. Zhang, G. Li, P. Zou, J. Zhang & N. Chi. High-speed visible light communication systems based on Si-substrate LEDs with multiple superlattice interlayers. *Photonix* **2021**, 2(1), 1-18.
14. J. Li, P. Zou, X. Ji, X. Guo & N. Chi. High-speed visible light communication utilizing monolithic integrated PIN array receiver. *Optics Communications* **2021**, 494, 127027.
15. Li, C., Chen, P., Li, J., Chen, K., Guo, C., & Liu, L. (2022). Modeling of thin-film lithium niobate modulator for visible light. *Optical Engineering*, 61(5), 057101-057101.
16. Y. Yang, C. Chen, P. Du, X. Deng, J. Luo, W.D. Zhong & L. Chen. Low complexity OFDM VLC system enabled by spatial summing modulation. *Optics Express* **2019**, 27(21), 30788-30795.
17. Y. Zhuang, L. Hua, L. Qi, J. Yang, P. Cao, Y. Cao & H. Haas. A survey of positioning systems using visible LED lights. *IEEE Communications Surveys & Tutorials* **2018**, 20(3), 1963-1988.
18. N. Chaudhary, O.I. Younus, L.N. Alves, Z. Ghassemlooy, S. Zvanovec & H. Le-Minh. An indoor visible light positioning system using tilted leds with high accuracy. *Sensors* **2021**, 21(3), 920.
19. W.X. Hong, J.Q. Wang & WZ Li. CSK hopping pattern model for visible light communication networks. *Optical and Quantum Electronics* **2019**, 51(4), 1-17.
20. J. Sebastián, D.G. Lamar, D.G. Aller, J. Rodriguez & PF. Miaja. On the role of power electronics in visible light communication. *IEEE J. Emerging and Selected Topics in Power Electronics* **2018**, 6(3), 1210-1223.
21. F. Wang, Y. Liu, F. Jiang & N. Chi. High-speed underwater visible light communication system based on LED employing maximum ratio combination with multi-PIN reception. *Optics Commun.* **2018**, 425, 106-112.
22. X. Wu, F. Hu, P. Zou, X. Lu & N. Chi. The performance improvement of visible light communication systems under strong non-linearities based on Gaussian mixture model. *Microwave and Optical Technology Letters* **2020**, 62(2), 547-554.
23. H. Freag, E.S. Hassan, S.A. El-Dolil & M.I. Dessouky. PAPR reduction for OFDM-based visible light communication systems using proposed hybrid technique. *Int. J. Communication Systems* **2018**, 31(10), e3582.
24. W.W. Hu. PAPR reduction in DCO-OFDM visible light communication systems using optimized odd and even sequences combination. *IEEE Photonics Journal* **2019**, 11(1), 1-15.
25. R. Ahmad & A. Srivastava, PAPR reduction of OFDM signal through DFT precoding and GMSK pulse shaping in indoor VLC. *IEEE Access* **2020**, 8, 122092-122103.
26. J. Ma, J. He, J. Shi, Z. Zhou & R. Deng, Non-linear compensation based on k-means clustering algorithm for Nyquist PAM-4 VLC system. *IEEE Photonics Technology Letters* **2019**, 31(12), 935-938.
27. J.K. Lain & Y.H. Chen. An ANN-based adaptive predistorter for LED non-linearity in indoor visible light communications. *Electronics* **2021**, 10(8), 948.
28. M. Abd Elkarim, M.M. Elsherbini, H.M. AbdelKader, & M.H. Aly, Exploring the effect of LED non-linearity on the performance of layered ACO-OFDM. *Applied Optics* **2020**, 59(24), 7343-7351.